International
Journal
Of Advanced Research in Engineering & Management (IJAREM)
ISSN: 2456-2033 || PP. 01-09

Experimental Study on Optimizing the Compressive Performance of Aluminum Alloy Circular Pipe Reinforced with Carbon Fiber

Zhao Peng, Yu Yong-ping, Tang Yu-xuan, Du Xing-gu, Sun Bo-yang, Luo Mao-rui, Chen Cong
College of Construction Engineering, Jilin University, Changchun, China

Abstract: In this paper, three kinds of carbon fiber cloth (CFRP) reinforcement schemes for aluminum alloy round tube are proposed, which are two ends reinforcement, section reinforcement and whole package reinforcement. The failure forms, load-displacement curves and stress-strain curves of aluminum alloy circular tubes reinforced by carbon fiber cloth were obtained through axial compression loading tests. The test results show that the yield strength and ultimate compressive strength of the aluminum alloy round tube strengthened by CFRP segment are superior to those of the aluminum alloy round tube strengthened by CFRP two ends and the aluminum alloy round tube strengthened by CFRP whole package. The yield strength and ultimate compressive strength of the aluminum alloy round tube strengthened by CFRP segment are increased by 17.79% and 7.76%, respectively, and the ultimate compressive strength values are increased by 2.09% and 1.93%, respectively. The ultimate displacement of the all-wrapped aluminum alloy tube is best among the three kinds of carbon fiber cloth, which is improved by 22.22% and 7.84%, respectively. Finally, by comparing the cost of aluminum alloy round pipe reinforced by CFRP segment with that of aluminum alloy round pipe reinforced by CFRP whole package, it is found that the cost of aluminum alloy round pipe reinforced by CFRP segment can be saved by 14.48%. The compression performance of aluminum alloy tube reinforced by CFRP segment is obviously improved and the cost is effectively saved.

Keywords: Carbon fiber cloth, Aluminum alloy round tube, Compressive strength, Strain, Cost

1. Introduction

Since the 1960s, fiber-reinforced polymer (FRP) composite materials have been used in civil engineering [1], and their light-weight and high-strength advantages have been widely used in repairing and upgrading reinforced engineering structures [2-3]. Many studies have shown that pasting FRP fabric onto metal surfaces has also developed into a metal strengthening method [4, 5], improving the physical properties of materials, including higher bearing capacity [6], stronger buckling resistance [7], longer service life [8], and greater energy absorption capacity [9]. Aluminum alloy materials and fiber polymers have similar advantages such as lightweight, corrosion resistance, non-ferromagnetism, and good plasticity. The combination of FRP and aluminum alloy materials retains these advantages and even exhibits improved behavior, including higher load-bearing capacity and stiffness compared to pure aluminum alloy materials, and better ductility compared to pure FRP. Due to these advantages, the application range of fiber polymer and aluminum alloy composite components has been further expanded, which can be applied to lattice shells, grid structures, suspension structures, folded plate structures, and membrane structures [10].

The method of strengthening aluminum alloy with FRP is a key factor affecting the properties of FRP aluminum alloy materials. The main forms of compression failure of aluminum alloy pipes are end-expansion or tearing and middle buckling [11-13]. At present, the main method of reinforcing metal pipes with FRP is to stick the FRP fabric onto the metal surface [14]. Triantafillou et al. [15] studied the bending performance of CFRP fully encapsulated aluminum alloy pipe composite components and found that the stiffness and load-bearing capacity of the composite material were significantly improved. Truong et al. [16] found that the tensile strength and failure strain of CFRP aluminum alloy composite specimens were significantly improved. Kim [17] analyzed the economic effects of CFRP aluminum alloy hybrid bending components and found that these components provide various economic advantages. The FRP fully wrapped aluminum alloy reinforcement scheme can significantly improve its physical properties, but there is still room for improvement in terms of economy.

A targeted CFRP segmented reinforcement plan for aluminum alloy pipes based on the three aspects of compression failure morphology, construction difficulty, and economy is proposed in this paper. This study designed three reinforcement schemes: end reinforcement, end and middle section reinforcement, and full package reinforcement. According to GBT7314-2017- Metal Compression Test Method [18], the optimization plan for CFRP-reinforced aluminum alloy pipes is compared in terms of compressive strength, stress-strain curve, elastic modulus, and other aspects.

2. Experimental plan and phenomena

2.1 Material properties

This article selects 6063-t5 aluminum alloy circular tube (thickness 3mm) and CFS-I-300 Class I 300g carbon fiber cloth (CFRP) (thickness 0.167mm) as the experimental materials. The mechanical properties of aluminum alloy materials are listed in Table 1, and the stress-strain is shown in Fig. 1. The mechanical properties of CFRP were determined according to the requirements of the Standard Test Method for Tensile Properties of Polymer Matrix Composite Materials (ASTMD3039/D3039M) [19], as shown in Table 2. The mechanical properties of epoxy resin as a CFRP bonding material are also listed in Table 2.

Table 1 Mechanical property parameters of aluminum alloys

Material	Yield strength	Tensile strength	Elastic modulus
Aluminum alloy	190.0MPa	217.3MPa	69.8GPa

Table 2 Mechanical properties of carbon fiber and epoxy resin mater

Material	Thickness	Tensile strength	Elastic modulus
CFRP	0.167mm	3532MPa	$2.33x10^5$MPa
Epoxy resin		>40MPa	>2800MPa

2.2 Sample preparation and reinforcement plan

According to GBT7314-1987- Metal Compression Test Method [18], compression tests are conducted on aluminum alloy pipes to determine their compressive strength. According to the requirement of standard [18], L=(5~8) d_0, it is a medium short column. In this article, an aluminum alloy pipe with a length of 300mm is used. CFRP is reinforced by attaching epoxy resin to the surface of aluminum alloy. The reinforcement scheme is shown in Fig. 2 and Table 3. The overlap length of CFRP is 40mm, and the epoxy resin adhesive are configured according to the ratio of epoxy resin and curing agent 10:3. After CFRP reinforcement, all specimens were placed in a dry and cool place (at a temperature of 25℃) for 7 days to ensure complete solidification of the epoxy resin. After the epoxy resin has completely solidified, the upper and lower surfaces of the specimen are polished to a flat surface, and the outer surface of the CFRP is wiped with acetone.

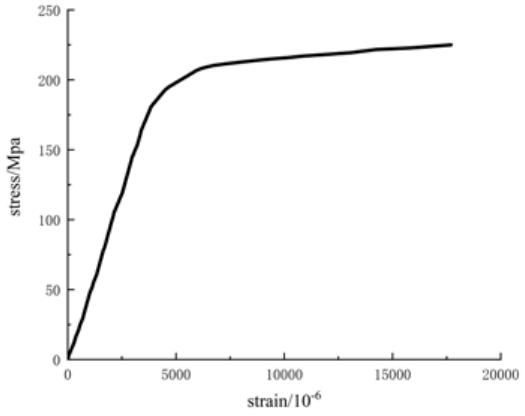

Fig. 1 Stress-strain relationship of aluminum alloys

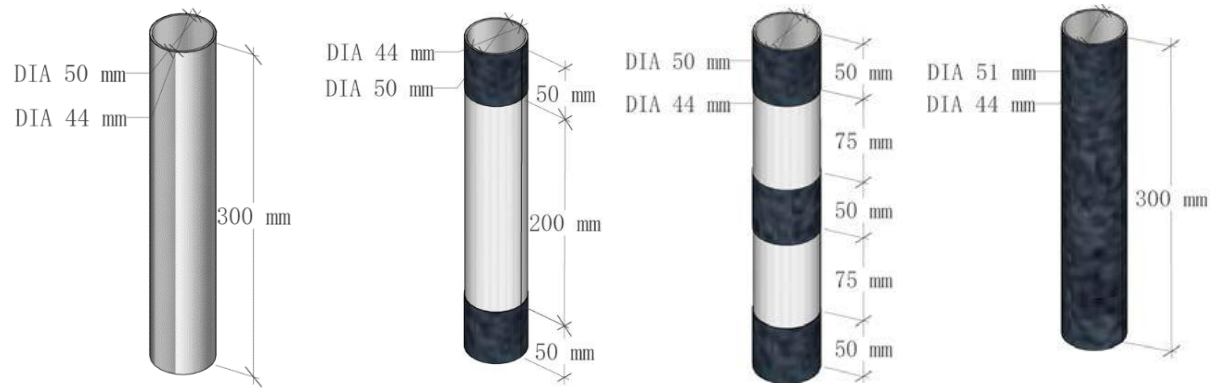

(a) Unreinforced (b) Reinforcement at both ends (c) Three-section reinforcement (d) All-inclusive reinforcement

Fig. 2 Reinforcement Plan for Aluminum Alloy Pipe with Carbon Fiber Cloth

2.3 Loading device and measurement point distribution

According to GBT7314-2017- Metal Compression Test Method [18], the controlled displacement method was used on aluminum alloy pipes, with a loading speed 3mm/min. To determine the stress-strain relationship of aluminum alloy pipes, strain gauges were attached at both ends and in the middle ofthe pipes. The strain gauge parameters are shown in Table 4. The specific sticking position of the strain gauge is shown in Fig. 3.

Table 3 Sample reinforcement plan

Pipe wall thickness	Test piece number	Reinforcement plan	Number of reinforcement layers
3mm	LC-1	Unreinforced（Fig. 2(a))	1
	LC-2	Reinforcement at both ends (Fig. 2(b))	1
	LC-3	Three section reinforcement (Fig. 2(c))	1
	LC-34	All inclusive reinforcement (Fig. 2(d))	1

Table 4 Basic parameters of strain gauges for testing

Model	Resistance	Sensitivity coefficient	Accuracy class
120-5AA-R-D150	120Ω	2.0±1%	A

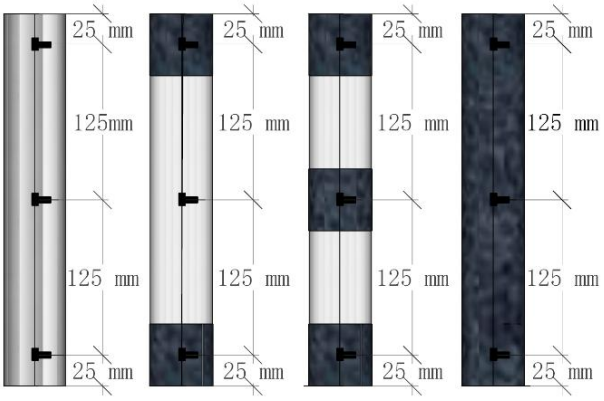

Fig. 3 Strain gauge bonding position

3. Test Results and Analysis

3.1 Failure mode of aluminum alloy circular tube

During initial loading, the vertical deformation of the specimen increases linearly with increasing load. When the load increases to about 80% of the material's ultimate load, the vertical deformation begins to increase nonlinearly, and the material enters the yield stage until convex deformation occurs near the end of the specimen. Afterward, the load slowly increased, but the bearing capacity of the reinforced aluminum alloy circular tube began to decrease until the specimen was damaged (Fig. 4). Before yielding, each sample exhibits good linearity. When the load approaches the yield load, the cracking sound of CFRP fiber fracture can be heard. After yielding, CFRP controls the buckling of the aluminum alloy circular tube, thereby delaying the final failure of the specimen and causing the axial load to continue to increase until the specimen fails.

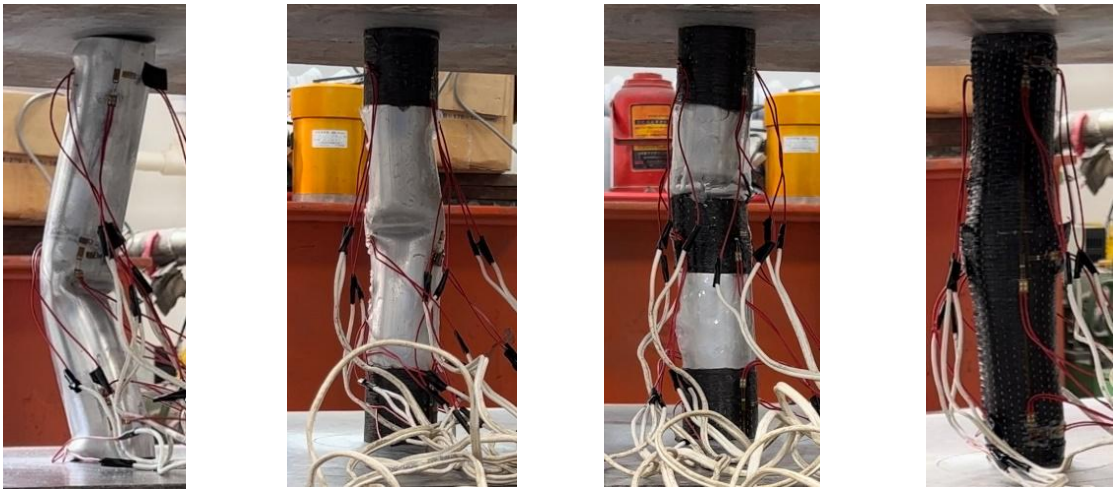

(a) Intermediate buckling (b) Middle and Elephant Foot Flexion (c) Buckling of non-reinforced sections (d) Intermediate drumbeat

Fig. 4 Failure morphology of aluminum alloy pipes

Different CFRP reinforcement methods for aluminum alloy circular pipes have different structural constraints, resulting in different axial bearing capacities and failure modes of the specimens. The LC-1 specimen first undergoes bulging at the upper end, then bends in the middle, and finally produces a corner at both ends (Fig. 4 (a)). The end bulging of CFRP-reinforced aluminum alloy circular tubes occurs in the bonding area between CFRP and aluminum alloy circular tubes (Fig. 4 (b) (c)). CFRP can effectively suppress the bulging of aluminum alloy circular tubes and delay the flexion of elephant feet. The middle part of LC-1 and LC-2 specimens experience buckling. However, the middle part of the LC-1 specimen exhibits significant deformation and exhibits good ductility. During the deformation of the middle part of the LC-2 specimen, the bonding zone between CFRP and aluminum alloy circular tube undergoes tearing failure. The unreinforced part of the aluminum alloy circular tube of LC-3 specimen is divided into two parts: upper and lower. The damaged buckling part of LC-3 specimen is only distributed in the upper or lower parts. The three-section reinforced aluminum alloy circular tube effectively constrains the lateral deformation of the aluminum alloy circular tube. The LC-4 specimen has the smallest lateral deformation, mainly due to middle bulging and CFRP fracture (Fig. 4 (d)). After yielding, the stiffness of the CFRP reinforcement sleeve remains high, which can provide stiffness for aluminum alloy circular pipes. Therefore, CFRP can suppress the outward protrusion of the yielding part of aluminum alloy circular tubes, preventing or delaying elephant foot buckling.

3.2 load-displacement curve

The axial load-displacement curves of the four types of specimens in this experiment are shown in Fig. 5. From the graph, it can be observed that the load displacement trend of aluminum alloy pipes can be divided into three stages: 1) in the elastic stage, the load-displacement shows a linear growth trend; 2) During the strengthening stage, the slope of the load-displacement curve gradually decreases and finally reaches the ultimate load; 3) During the failure stage, the load-displacement curve gradually decreases until failure occurs. In the elastic stage, the trend of the load-displacement curve of reinforced aluminum alloy pipes is significantly

slower than that of unreinforced loads, with a smaller slope. Comparing the slope of the load-displacement curve of the reinforced specimens in the elastic stage, the effect of CFRP reinforcement on aluminum alloy pipe specimens is LC-3>LC-4>LC-2>LC-1. This proves that the effect of three-stage reinforcement in the elastic stage is better than that of full-package reinforcement and two-end reinforcement. In the strengthening stage, the trend of the load-displacement curve of the reinforced specimen is flat, and the extended displacement is better than that of the unreinforced specimen.

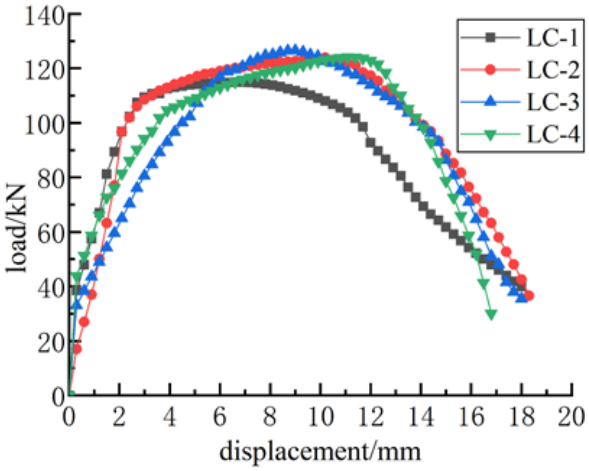

Fig. 5 load-displacement curve

Combining the compressive strength and vertical displacement of the specimen, the analysis was conducted using the average values of two sets of experimental results, as shown in Table 5. The yield strength, compressive strength, yield displacement, and ultimate displacement of the reinforced specimen are better than those of the unreinforced specimen (LC-1). The yield strength of the three-stage reinforcement (LC-3) specimen is significantly better than that of the other two types of reinforcement (LC-2, LC-4) specimens, with values of 113.9kN, 96.7kN, and 105.7kN, respectively. Meanwhile, the ultimate load of the three-section reinforced specimens is 126.5kN, 123.9kN, and 124.1kN, respectively, compared to the other two types of reinforced specimens. However, the ultimate compressive strength of LC-3 is not significantly improved compared to LC-2 and LC-4, with 2.09% and 1.93% respectively. The yield strength, compressive strength, yield displacement, and ultimate displacement of the LC-4 specimen are superior to those of the LC-2 specimen reinforced at both ends. However, comparing the ultimate displacement, the LC-4 specimen performs the best compared to LC-2 and LC-3 specimens, with values of 11.1mm, 9.0mm, and 10.2mm, respectively. All-inclusive specimens have excellent ductility.

Table 5 Compressive strength and vertical displacement of the specimen

Test piece number	Elastic stage		Strengthening stage	
	Yield load	Displacement	Ultimate load	Displacement
LC-1	89.3kN	1.8mm	114.9kN	6.9mm
LC-2	96.7kN	2.1mm	123.9kN	10.2mm
LC-3	113.9kN	5.7mm	126.5kN	9.0mm
LC-4	105.7kN	4.2mm	124.1kN	11.1mm

3.3 Analysis of load strain curve of specimen

From Figs. 6 (a), (b), (c), and (d), LC-1 is linear elastic in its initial stage until the stress reaches the non-proportional elongation strength. Its own longitudinal and circumferential strains first increase in the middle part, followed by both sides, which is more consistent with its failure mode. There is a significant mutation in the lower longitudinal strain of LC-1. The longitudinal and circumferential strains in the middle part of the LC-2 specimen first increase and grow rapidly, while the longitudinal and circumferential strains in the reinforced parts at both ends grow slower than those in the unreinforced parts, which is consistent with the failure mode. The circumferential and longitudinal strains in the middle part of the LC-2 specimen are significantly greater

than those in the upper and lower parts. The longitudinal and circumferential strains at both ends of the LC-3 specimen increase rapidly, while the longitudinal and circumferential strains in the middle part do not increase significantly, which is consistent with its failure mode. The LC-4 specimen also exhibits the above trend, but it is not significant. In the elastic stage, there is little difference in the trend of load strain curves between the upper, middle, and lower parts of the specimen itself. The reinforcement of different parts of aluminum alloy pipes with CFRP has no significant impact on the longitudinal and circumferential strains of different parts.

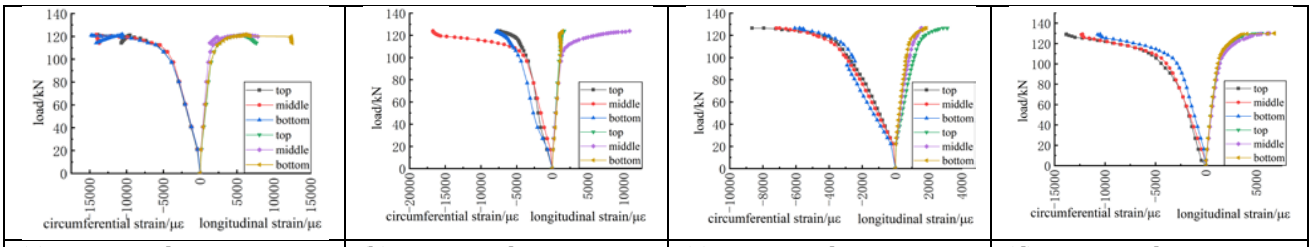

(a) LC-1 Load strain curve | (b) LC-2 Load strain curve | (c) LC-3 Load strain curve | (d) LC-4 Load strain curve

Fig. 6 Load strain curve

3.4 Analysis of load vertical strain curve

Comparisons of the longitudinal strains in the upper, middle, and lower parts of specimens with different reinforcement methods, are as shown in Fig. 7 (a), (b) and (c). Overall, the longitudinal strain of the unreinforced specimens varies significantly with increasing load. Under the same load conditions, the three-section reinforced specimen (LC-3) and the fully enclosed specimen (LC-3) effectively restrained the longitudinal displacement changes of the upper, lower, and middle aluminum alloy pipes. There is a sudden change in the longitudinal strain at both ends of the LC-1 specimen, which is reinforced at both ends. Due to CFRP. Comparing the restraining effect of CFRP on longitudinal strain of aluminum alloy pipes, LC-3>LC-4>LC-2>LC-1.

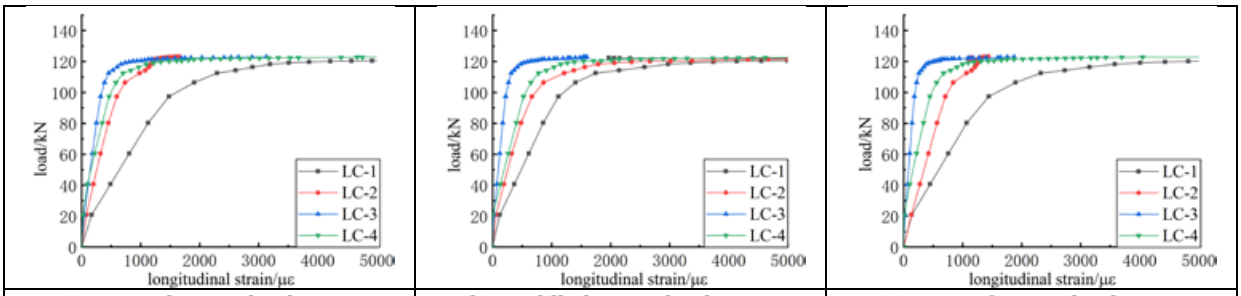

(a) Upper longitudinal strain comparison | (b) Middle longitudinal strain comparison | (c) Lower longitudinal strain comparison

Fig 7 Longitudinal load strain curve

3.5 Analysis of load circumferential strain curve

Figures 8 (a), (b), and (c) show the load circumferential strain curves of CFRP-reinforced aluminum alloy pipes at the same location. In Figs. 8 (a) and (b), the slope of CFRP in the upper and middle parts of the specimen towards the load circumferential strain curve of aluminum alloy pipes is LC-1>LC-2>LC-4>LC-3. Thus, it has been proven that CFRP has a restraining effect on the circumferential strain of aluminum alloy pipes LC-3>LC-4>LC-2>LC-1. However, the circumferential strain in the lower part of the specimen (Fig. 8 (c)) shows a very similar trend in LC-3 and LC-4. The segmented reinforcement of CFRP aluminum alloy pipes can effectively control the circumferential deformation of the pipes, and its overall effect is better than that of CFRP fully wrapped aluminum alloy pipes.

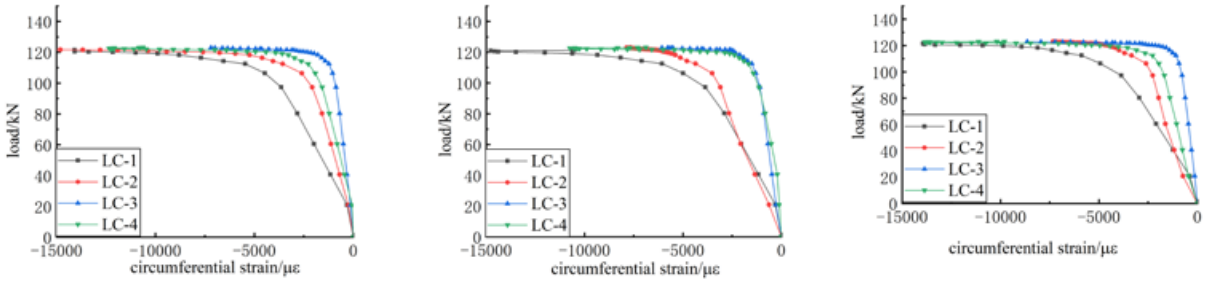

(a) Circumferential strain upper part (b) Middle of circumferential strain (c) Circumferential strain lower part

Fig. 8 Circumferential load strain curve

3.6 Elastic modulus analysis

According to the formula 1 for calculating the elastic modulus *Ec*in GBT7314-2017 Metal Compression Test Method [18]:

$$E_c = \frac{(F_k - F_j)L_0}{(\Delta L_k - \Delta L_j)S_0} \quad (1)$$

The parameter *Fj* is the bearing load when controlling the longitudinal displacement $\Delta L_j$and $F_k$is the bearing load when controlling the longitudinal displacement ΔL_k, L_0specimen length, S_0cross-sectional area of the specimen.

The elastic modulus of aluminum alloy pipe specimens can be calculated and displayed in Table 6. The relationship $E_{(LC\text{-}1)c} > E_{(LC\text{-}2)c} > E_{(LC\text{-}4)c} > E_{(LC\text{-}3)c}$, which proves that CFRP effectively constrains the longitudinal displacement of aluminum alloy pipes under axial pressure, with segmented CFRP reinforcement having the best effect. However, compared to the full reinforcement of aluminum alloy pipes, the effect of segmented CFRP reinforcement on aluminum alloy pipes is not significantly improved, at 0.42%.

Table 6 Elastic modulus

Test-Piece	Bearing Load (kN)	Control Longitudinal Displacement (mm)	Bearing Load (kN)	Control Longitudinal Displacement (mm)	Test Piece Length (mm)	Cross-Sectional Area of Specimen (mm2)	Elastic Modulus of Specimen (GPa)
LC-1	60.5	3.00	106.4	3.90	300	442.9	67.7
LC-2	37.0	2.56	102.0	3.85	300	442.9	66.9
LC-3	43.6	0.78	102.3	1.98	300	442.9	67.2
LC-4	26.8	1.56	100.5	3.06	300	442.9	66.6

3.7 Carrying capacity and cost analysis

Combining the analysis of failure morphology, load-displacement curve, load strain curve, and elastic modulus, CFRP-reinforced aluminum alloy pipes can effectively improve the compressive strength and ductility of aluminum alloy pipes, and constrain the longitudinal and circumferential deformation of aluminum alloy pipes. Among them, the segmented reinforcement effect of CFRP on aluminum alloy pipes is better than the other two reinforcement methods. However, the improvement compared to the CFRP fully reinforced aluminum alloy pipe specimens is very small.

Although the compressive strength of CFRP segmented reinforced aluminum alloy pipes is slightly higher than that of CFRP fully reinforced aluminum alloy pipe specimens. Based on the construction difficulty and material cost, the cost of CFRP segmented reinforcement and fully reinforced aluminum alloy pipes is calculated, as shown in Eqs. (2) – (4). The amount of CFRP reinforcement material used per unit length of aluminum alloy pipes in the CFRP segmented reinforcement plan is half of the total CFRP reinforcement plan. However, the construction difficulty of the CFRP segmented reinforcement scheme is 1.5 times that of the

CFRP fully inclusive reinforcement scheme. This indicates that the construction time of the CFRP segmented reinforcement scheme is 1.5 times that of the CFRP full package reinforcement scheme.

$$C_{total} = C_{construction} + C_{material} \quad (2)$$

$$C_{material} = C_{CFRP} + C_{Epoxy} \quad (3)$$

$$C_{construction} = C_h \text{ X } h \quad (4)$$

The cost calculation of the CFRP segmented reinforcement scheme and the CFRP full package reinforcement scheme in this experiment is shown in Table 7.

The above calculation represents the cost of the 30cm specimen used in the experiment. The segmented reinforcement cost scheme saved 11% compared to the full package reinforcement scheme. Compared to the full package reinforcement scheme, the segmented reinforcement cost scheme saves 14.48% with 300cm aluminum alloy pipes. Therefore, without reducing the compressive strength reinforcement effect of aluminum alloy pipes, the segmented reinforcement scheme can greatly save costs.

Table 7 Cost calculation for CFRP reinforcement

Reinforcement plan	CFRP cost	Epoxy resin cost	Construction duration
CFRP segmented reinforcement	￥3.5	￥2.95	0.25h
CFRP all-inclusive reinforcement	￥6.00	￥5.78	0.17h

4. Conclusions

Two-end reinforcement, segmented reinforcement, and full-package reinforcement schemes for the axial compression failure state of aluminum alloy pipes are presented. By comparing the compression failure states of three types of CFRP-reinforced aluminum alloy pipes, the deformation part of the segmented CFRP-reinforced aluminum alloy pipe is in the unreinforced part, and the failure part is in a part of the unreinforced aluminum alloy pipe, effectively protecting the overall integrity of the aluminum alloy pipe. Comparing the yield strength and ultimate strength of three types of CFRP-reinforced aluminum alloy pipes, the yield strength of the three-section reinforced (LC-3) specimen is significantly better than the other two types of reinforced (LC-2, LC-4) specimens, with an increase of 17.79% and 7.76%, respectively. The ultimate compressive strength of LC-3 is not significantly improved compared to LC-2 and LC-4, with 2.09% and 1.93% respectively. However, the ultimate displacement of LC-4 is higher than that of LC-2 and LC-3, but the improvement is not significant, at 22.22% and 7.84%, respectively. By analyzing the load strain curve and elastic modulus, it can be concluded that the reinforcement effect of aluminum alloy pipes is LC-3>LC-4>LC-2>LC-1. However, the improvement in segmented reinforcement compared to full package reinforcement is very small. On the other hand, from the perspective of cost control, the segmented reinforcement scheme has saved about 14.48% compared to the full-package reinforcement scheme, effectively controlling costs. Therefore, this article suggests that the segmented reinforcement scheme is suitable for the reinforcement of aluminum alloy pipes. Further experimental research is needed to verify the effectiveness of other segmented reinforcement schemes in improving the bearing capacity and cost control of aluminum alloy pipes.

Acknowledgments

This work is supported by the National Natural Science Foundation of China (Grant No. 42372356 and 41972323)

References

[1]. Zhao X L, Zhang L. State-of-the-art review on FRP strengthened steel structures. Engineering Structures, *29(8)*, 2007, 1808-1823.

[2]. Ye L P, Feng P. Applications and development of fiber-reinforced polymer in engineering structures. *China Civil Engineering Journal, 2006(003)*, 039.

[3]. Alajarmeh O S, Manalo A C, Benmokrane B, et al. Hollow concrete columns: Review of structural behavior and new designs using GFRP reinforcement. *Engineering Structures, 203*, 2020, 109829.

[4]. Feng P, Hu L L, Qian P, Ye L P. Compressive bearing capacity of CFRP–aluminum alloy hybrid tubes. *Composite Structures, 140,* 2016, 749-757.

[5]. Zhang X Q, Jiang S C. Overview of FRP Strengthening and Repairing Metal Structures. *Journal of Civil Engineering and Management, 31(02),* 2014, 39-50.

[6]. Feng P, Cheng S, Bai Y, et al. Mechanical behavior of concrete-filled square steel tube with FRP-confined concrete core subjected to axial compression. *Composite Structures, 123,* 2015, 312-324.

[7]. Guades E, Aravinthan T, Manalo A, et al. Experimental investigation on the behavior of square FRP composite tubes under repeated axial impact. *Composite Structures, 97,* 2013, 211-221.

[8]. Aakkula J, Saarela O. An experimental study on the fatigue performance of CFRP and BFRP repaired aluminum plates. *Composite Structures, 118,* 2014, 589-599.

[9]. Kalhor R, Case S W. The effect of FRP thickness on energy absorption of metal-FRP square tubes subjected to axial compressive loading. *Composite Structures, 130,* 2015, 44-50.

[10]. Pantelides C P, Nadauld J, Cercone L. Repair of Cracked Aluminum Overhead Sign Structures with Glass Fiber Reinforced Polymer Composites. *Journal of Composites for Construction, 7(2),* 2015, 118-126.

[11]. Cui G, Meng L, Zhai X. Buckling behaviors of aluminum foam-filled aluminum alloy composite columns under axial compression. *Thin-Walled Structures,* 2022, 177.

[12]. Li Z, Yang H, Hu X, et al. Experimental study on the crush behavior and energy-absorption ability of circular magnesium thin-walled tubes and the comparison with aluminum tubes. *Engineering Structures, 164,* 2018, 1-13.

[13]. Liu M, Zhang L, Wang P, et al. Buckling behaviors of section aluminum alloy columns under axial compression. *Engineering Structures, 95,* 2015, 127-137.

[14]. Feng P, Hu L L, Qian P, Ye L P. Buckling behavior of CFRP-aluminum alloy hybrid tubes in axial compression. *Engineering Structures, 132,* 2017, 624-636.

[15]. Triantafillou T C, Kim P, Meier U. Optimization of hybrid aluminum/CFRP box beams. *International Journal of Mechanical Sciences, 33(9),* 1991, 729-739.

[16]. Truong G T, Hai V T, Choi K K. Tensile behavior of on- and off-axis carbon fiber reinforced polymer composites incorporating steel wire mesh. *Mechanics of materials, 137,* 2019, 103131.

[17]. Kim P. A. Comparative Study of the Mechanical Performance and Cost of Metal, FRP, and Hybrid Beams. *Applied Composite Materials, 5(3),* 1998, 175-187.

[18]. *Experimental method for room temperature compression of metallic materials: GBT7314-2017.* (Beijing, China Construction Industry Press, 2017)

[19]. *ASTM C39. Standard Test Method for Tensile Properties of Polymer Matrix Composite Materials.* (West Conshohocken (PA), ASTM International, 2018)